

# Fluid Antenna System: New Insights on Outage Probability and Diversity Gain

Wee Kiat New, *Member, IEEE*, Kai-Kit Wong, *Fellow, IEEE*, Xu Hao, *Member, IEEE*, Kin-Fai Tong, *Fellow, IEEE*, and Chan-Byoung Chae, *Fellow, IEEE*

## Abstract

To enable innovative applications and services, both industry and academia are exploring new technologies for sixth generation (6G) communications. One of the promising candidates is fluid antenna system (FAS). Unlike existing systems, FAS is a novel communication technology where its antenna can freely change its position and shape within a given space. Compared to the traditional systems, this unique capability has the potential of providing higher diversity and interference-free communications. Nevertheless, the performance limits of FAS remain unclear as its channels and system properties are highly peculiar to be analyzed. To address this, we approximate the outage probability and diversity gain of FAS in closed-form expressions. We then propose a suboptimal FAS with  $N^*$  ports, where a significant gain can be obtained over FAS with  $N^* - 1$  ports whilst FAS with  $N^* + 1$  ports only yields marginal improvement over the proposed suboptimal FAS. In this paper, we also provide analytical and simulation results to unfold the key factors that affect the performance of FAS. Limited to systems with one active radio frequency (RF)-chain, we show that the proposed suboptimal FAS outperforms single-antenna (SISO) system and selection combining (SC) system in terms of outage probability. Interestingly, when the given space is  $\frac{\lambda}{2}$ , the outage probability of the proposed suboptimal FAS with one active RF-chain achieves near to that of the maximal ratio combining (MRC) system with multiple active RF-chains.

## Index Terms

6G, fluid antenna system, outage probability, diversity gain, performance analysis.

The work is supported by the Engineering and Physical Sciences Research Council (EPSRC) under grant EP/W026813/1. For the purpose of open access, the authors will apply a Creative Commons Attribution (CC BY) licence to any Author Accepted Manuscript version arising. (Corresponding author: Kai-Kit Wong)

Wee Kiat New (email: a.new@ucl.ac.uk), Kai-Kit Wong (email: kai-kit.wong@ucl.ac.uk), Xu Hao (email: hao.xu@ucl.ac.uk), and Kin-Fai Tong (email: k.tong@ucl.ac.uk) are with the Department of Electronic and Electrical Engineering, University College London, London WC1E 6BT, United Kingdom.

Kai-Kit Wong and Chan-Byoung Chae (email: cbchae@yonsei.ac.kr) are with School of Integrated Technology, Yonsei University, Seoul, Korea.

## I. INTRODUCTION

Fifth generation (5G) wireless networks have recently been deployed worldwide and thus the industry and academia are now looking for new technologies to maximize the potentials of sixth generation (6G) wireless networks. One of the promising candidates is fluid antenna system (FAS). Unlike traditional antenna systems, FAS is a software-controllable fluidic, conductive, or dielectric structure that can freely adjust its position and shape within a given space [1].

For example, the most basic single fluid antenna consists of one radio frequency (RF)-chain and  $N$  ports that are distributed in a given space. The radiating element of the fluid antenna can freely switch its position among the ports (e.g., the strongest port) to obtain a stronger channel gain, lower interference, and other desirable performance [2]. This is achievable due to the recent advancement of using liquid metals (e.g., Galistan and Eutectic Gallium Indium) and ionized solutions (e.g., sodium chloride and potassium chloride) for antennas. Note that software-controlled pixel antennas, moveable antennas and other flexible antenna structures are also considered as fluid antenna [3]. Besides, FAS can co-exist with other 6G candidates such as re-configurable intelligent surfaces [4], surface-wave communications [5], intelligent massive multiple-input multiple-output [6], and terahertz communications [7].

Despite its advantages, the fundamental limits of FAS and key factors that affect its performance remain unclear. One of the reasons is because the channels of FAS are strongly correlated since the ports can be closely placed to each other. Consequently, the probability density function (PDF) and cumulative distribution function (CDF) of FAS channels are intractable [8]. As a result, the outage probability and diversity gain of FAS are not known in closed-form expressions. In addition, increasing the number of ports of FAS has an inherent diminishing gain due to one active RF-chain [9].<sup>1</sup> Thus, a suboptimal number of ports that are required to achieve a satisfactory performance is not known. Yet, this number is practically and theoretically important as it reduces the implementation challenges and analysis complexity.

Researchers might argue that FAS resembles a traditional selection combining (SC) system as the strongest antenna is selected in a point-to-point setting. From this viewpoint, some similarities are observed as there is a set of antennas/ports to select from and both systems only use one active RF-chain for communications. Nevertheless, FAS can have infinitely many ports (e.g.,

<sup>1</sup>Throughout this paper, we refer to an active RF-chain as the RF-chain used for communications. In contrast, the term RF-chains refers to a collection of RF-chains that are connected to each antenna for it to work as intended.

when using liquid metals) which makes the implementation and analysis much more challenging. In addition, the unique capability of freely switching the radiating element among the ports can be exploited to mitigate multi-user interference. These features are impractical or too costly in traditional SC systems.

State-of-the-arts show that FAS outperforms maximal ratio combining (MRC) system if the number of ports is sufficiently large [3]. In fact, [3] proves that FAS achieves arbitrarily small outage for a fixed rate/signal-to-noise ratio (SNR) as  $N \rightarrow \infty$ . In [10], the authors reveal that the ergodic capacity of FAS increases with  $N$  and thus FAS can outperform MRC in terms of ergodic capacity. Interestingly, FAS can also be used for multiple access. Specifically, [11] proposes a fluid antenna multiple access (FAMA) system which leverages the moment of deep fades in space to reduce multi-user interference. Motivated by these works, [12] employs stochastic geometry to analyze the outage probability of FAS in large-scale downlink cellular networks and [13] analyzes the performance of FAS in a more general correlated fading channel.

Nevertheless, [14] alludes that the channel modeling in the previous works might be inaccurate. To address this, [8] proposes a highly complicated channel model to follow closely the spatial correlation of the Jake's model. Using this channel model, they highlight that FAS has limited performance gain as  $N$  increases. Yet, the key reasons that limit the performance of FAS remain ambiguous. This is because the eigenvalue and eigenvector entries that are used in the analytical PDF/CDF expressions provide limited insights.

It is important to highlight that deriving the PDF/CDF of FAS channels is extremely challenging [8]. This is because the channels of FAS are strongly correlated and thus they have to be formulated in terms of multivariate distributions. Over the past few decades, extensive efforts have been dedicated to this problem [15]. However, most of the works only obtain the bivariate [16], [17], trivariate [16], [18], [19], or quadivariate [19], [20] distributions while other works restrict the correlation matrix to certain forms (e.g., equally correlated [21] and exponentially correlated [22]). Fortunately, the multivariate PDF/CDF of arbitrarily correlated Rayleigh distributions are recently derived in [23]–[25]. Nevertheless, the assumption of non-singular correlation matrix is retained. In this paper, we omit this assumption (i.e., our correlation matrix could be near-singular) and address the computation problem via a suboptimal approximation.<sup>2</sup>

<sup>2</sup>The computational problem of a near-singular correlation matrix is much harder to address than that of a singular matrix. This is because we can obtain an independent matrix from a singular matrix by removing the dependent entries [26]. But in the near-singular case, this approach cannot be applied. Instead, we need to rely on approximations.

In addition to the above works, [27] develops a port selection algorithm that can approach the performance of optimal FAS when only the received SNR of a few ports are observed. Furthermore, [28] considers a field-response channel model while omitting the spatial correlation effect and [29] extends the model to a multiple-input multiple-output (MIMO) scenario. Moreover, FAMA can be categorized into i) slow-FAMA and ii) fast-FAMA. The former switches its port when the channel changes [30] while the latter switches its port on a symbol-by-symbol basis [31]. The analytical outage probability of two-user FAMA is also derived in [32].

Motivated by the aforementioned works, this paper aims to understand the fundamental limits of FAS as well as the key factors that affect its performance. To this end, we approximate the outage probability and diversity gain of FAS in closed-form expressions via a simple and accurate channel model that follows closely the spatial correlation of Jake's model. In addition, we propose a suboptimal FAS with  $N^*$  ports as well as an algorithm to approximate  $N^*$ . The main contributions of our paper are summarized as follows:

- We employ a simple and accurate channel model that follows the spatial correlation of Jake's model. Based on this channel model, we approximate the outage probability in closed-form expressions. By applying Taylor series approximation, we simplify the outage probability at high SNR into a simpler and more meaningful expression. Using this result, we also obtain the diversity gain of FAS.
- We propose a suboptimal FAS with  $N^*$  ports. The proposed suboptimal FAS plays an important role as it enables FAS to achieve near-optimal performance with minimal number of ports. In particular, one may define  $\varepsilon_{\text{tol}}$  to adjust the sub-optimality of the proposed FAS. For example, if  $\varepsilon_{\text{tol}}$  is small, the proposed FAS is quantifiably near-optimal at a cost of more ports. In addition, we develop a polynomial-time algorithm to approximate  $N^*$ . Besides,  $N^*$  can be used to address the near-singular correlation matrix problem.
- We provide analytical and simulation results to demonstrate the key parameters that affect the performance of FAS. Our discussions include intuitive insights on the system characteristics as well as practical guidelines for efficient FAS design.

The rest of the paper is organized as follows: Section II details the system model and performance metrics. Section III presents the outage probability and diversity gain of FAS. The details of suboptimal FAS and the algorithm to approximate  $N^*$  are discussed in Section IV. Section V provides our numerical results and we conclude the paper in Section VI.

*Notations:* Scalar variables are denoted by italic letters (e.g.,  $c$ ), vectors are denoted by boldface

italic small letters (e.g.,  $c$ ) and matrices are denoted by boldface italic capital letters (e.g.,  $C$ ). Besides,  $(\cdot)^T$  denotes transpose,  $(\cdot)^H$  denotes conjugate transpose while  $|\cdot|$  and  $\|\cdot\|_F$  denotes absolute and Frobenius norm, respectively. Throughout this paper,  $\log(\cdot)$  denotes logarithm with base 2,  $\mathbb{E}[\cdot]$  denotes the expectation and  $\mathbb{P}\{\cdot\}$  denotes the probability of an event. In addition,  $f_c(\cdot)$  denotes the PDF of  $c$ , and  $F_c(\cdot)$  denotes the CDF of  $c$ . The notation  $\mathbf{1}_c\{\cdot\}$  is an indication function for condition  $c$  and  $[\cdot]_c^{+/-}$  outputs the argument that is lower/upper bounded by  $c$ .

## II. SYSTEM MODEL

In this paper, we consider a point-to-point FAS where the transmitter is equipped with a conventional antenna and the receiver is equipped with a fluid antenna. The fluid antenna consists of  $N$  ports, which are evenly distributed along a linear dimension of length  $W\lambda$  where  $\lambda$  is the wavelength of the operating system. Since the ports are closely packed together, there is a strong spatial correlation among them. Based on Jake's model [33], the spatial correlation between the  $m$ th and  $n$ th ports is given by

$$J_{m,n} = \sigma^2 J_0 \left( 2\pi \frac{(m-n)W}{N-1} \right), \quad (1)$$

where  $\sigma^2$  accounts for the large-scale fading effect and  $J_0(\cdot)$  is the zero-order Bessel function of the first kind.

For ease of analysis, we introduce the correlation matrix  $\mathbf{J}$  where

$$\mathbf{J} = \begin{bmatrix} J_{1,1} & \cdots & J_{1,N} \\ \vdots & \ddots & \vdots \\ J_{N,1} & \cdots & J_{N,N} \end{bmatrix}. \quad (2)$$

In (2), we have  $J_{m,n} = J_{n,m}$ . Therefore, using eigenvalue decomposition, we can obtain  $\mathbf{J} = \mathbf{U}\mathbf{\Lambda}\mathbf{U}^H$  where  $\mathbf{U}$  is an  $N \times N$  matrix whose  $n$ -th column (denoted by  $\mathbf{u}_n$ ) is the eigenvector of  $\mathbf{J}$  and  $\mathbf{\Lambda} = \text{diag}(\lambda_1, \dots, \lambda_N)$  is an  $N \times N$  diagonal matrix whose  $n$ -th diagonal entries are the corresponding eigenvalues of  $\mathbf{u}_n$ . Without loss of generality, we assume that the values of the eigenvalues in  $\mathbf{\Lambda}$  are arranged in descending order. i.e.,  $\lambda_1 \geq \dots \geq \lambda_N$ .

Throughout this paper, we assume there is only one RF chain in FAS and thus only one port can be activated for communications. The received signal of the  $n$ th port is expressed as

$$y_n = h_n x + w_n, \quad n = 1, \dots, N, \quad (3)$$

where  $h_n$  is the complex channel coefficient of the  $n$ th port,  $x$  is the information signal with  $\mathbb{E}[|x|^2] = P$  and  $w_n \sim \mathcal{CN}(0, N_0)$ ,  $\forall n$  is the additive white Gaussian noise of the  $n$ th port. Due to the spatial correlation of the ports,  $h_n$  can be modeled as

$$h_n = \sum_{m=1}^N u_{n,m} \sqrt{\lambda_m} z_m, \quad (4)$$

where  $u_{n,m}$  is the  $(n, m)$ -th entry of  $\mathbf{U}$ ,  $z_n = a_n + jb_n$ , where  $a_n, b_n, \forall n$ , are i.i.d. Gaussian random variables with zero mean and variance of  $\frac{1}{2}$ . According to [8], (4) can also be approximated as

$$\hat{h}_n = \Psi v_n + \sum_{m=1}^{\epsilon\text{-rank}} u_{n,m} \sqrt{\lambda_m} z_m, \quad (5)$$

where  $\epsilon\text{-rank}$  is a modeling parameter,  $\Psi = \sqrt{\sigma^2 - \sum_{m=1}^{\epsilon\text{-rank}} u_{n,m}^2 \lambda_m}$ ,  $v_n = c_n + jd_n$  and  $c_n, d_n, \forall n$ , are i.i.d. Gaussian random variables with zero mean and variance of  $\frac{1}{2}$ .

To obtain the global optimum performance, FAS activates a port with the maximum signal envelope [3],<sup>3</sup> i.e.,

$$|h_{\text{FAS}}| = \max\{|h_1|, \dots, |h_N|\}. \quad (6)$$

The average received SNR of the receiver is found as

$$\Theta = |h_{\text{FAS}}|^2 \frac{P}{N_0} = |h_{\text{FAS}}|^2 SNR, \quad (7)$$

where  $SNR = \frac{P}{N_0}$  is the transmit SNR and its outage probability is defined as

$$\mathbb{P}\{\log(1 + \Theta) < q\} = \mathbb{P}\{|h_{\text{FAS}}| < \Omega\}, \quad (8)$$

where  $\Omega = \sqrt{\frac{2^q - 1}{SNR}}$  and  $q$  is the minimum required rate. In addition, the diversity gain of FAS can be defined as [34]

$$\lim_{SNR \rightarrow \infty} -\frac{\log \mathbb{P}_e(SNR)}{\log(SNR)} \stackrel{(a)}{=} \lim_{SNR \rightarrow \infty} -\frac{\log \mathbb{P}\{\log(1 + |h_{\text{FAS}}|^2 SNR) < q\}}{\log(SNR)} = d, \quad (9)$$

where (a) follows from the fact that error probability and outage probability differ by a constant shift at high SNR [35].

<sup>3</sup>Due to the port spatial correlation, it is shown in [30] that only a small number of observed ports/training is required to obtain the full channel state information.

### III. OUTAGE PROBABILITY AND DIVERSITY GAIN OF FAS

As it is seen in (4), the complex channel coefficients  $\mathbf{h} = [h_1, \dots, h_N]^T$  are correlated. Therefore,  $|\mathbf{h}|$  is a correlated Rayleigh random vector. We present the following lemmas to obtain the closed-form outage probability and diversity gain of FAS.

**Lemma 1.** *The PDF of  $|\mathbf{h}|$  can be approximated as*

$$f_{|\mathbf{h}|}(r_1, \dots, r_N) \approx \eta \sum_{s_1=0}^{s_0} \sum_{s_2=0}^{s_1} \dots \sum_{s_T=0}^{s_{T-1}} \left(\frac{1}{2}\right)^{\sum_{t=1}^T s_t^*} \prod_{t=1}^T \beta(t, s_t^*) \sum_{\mathbf{v} \in \mathcal{V}} \left[ \prod_{t=1}^T \binom{s_t^*}{v_t} \right] \left[ (2\pi)^N \prod_{i=1}^N \mathbf{1}_{\{\Delta_i=0\}} \right]. \quad (10)$$

*Proof:* See Appendix A. ■

In (10),  $\eta = \frac{\prod_{n=1}^N |h_n|}{\pi^N \det(\mathbf{J})} \exp \left\{ -\frac{\sum_{n=1}^N |h_n|^2 K_{n,n}}{\det(\mathbf{J})} \right\}$ ,  $T = \frac{N(N-1)}{2}$ ,  $\beta(t, s_t) \triangleq \frac{\zeta_t^{s_t}}{s_t!}$ ,  $\zeta_t = -\frac{2K_{m,n}|h_n||h_m|}{\det(\mathbf{J})}$ , and  $s_t^* = s_t - s_{t+1}$  with  $s_{T+1} = 0$ . The subscript  $t$  and  $m, n$  are related as follows:  $t = n + (m-1)N - \frac{m(m+1)}{2}$ ,  $m < n$ , while  $m, n$  can be obtained from  $t$  with  $m = \min m' \in \mathbb{Z}$  subject to  $\sum_{i=1}^{m'} (N-i) > t$  and  $n = t - (m-1)N + \frac{m(m+1)}{2}$ .

Note that  $s_0$  is a finite constant which has to be large for the approximation to be accurate. In addition,  $\mathbf{v} = [v_1, \dots, v_T]^T$ ,  $\mathcal{V}$  denotes the set of all the possible permutations, and  $\Delta_i = \sum_{n=1}^N G_{i,n} + \sum_{n=1}^N G_{n,i} - G_{i,i}$ . Furthermore,  $K_{m,n}$  is the  $(m, n)$ -th entry of  $\mathbf{K}$  where  $\mathbf{K}$  is the co-factor of  $\mathbf{J}$ , and  $G_{m,n}$  is the  $(m, n)$ -th entry of  $\mathbf{G}$  where  $\mathbf{G}$  is defined as

$$\mathbf{G} = \begin{bmatrix} 0 & \gamma_1 & \gamma_2 & \cdots & \gamma_{N-1} \\ & & \gamma_N & \cdots & \gamma_{2N-3} \\ \vdots & \ddots & & \ddots & \\ & & & & \gamma_T \\ 0 & \cdots & & & 0 \end{bmatrix}, \quad (11)$$

and  $\gamma_t = 2v_t - j_t^* \in \mathbb{Z}$ .

**Lemma 2.** *The CDF of  $|\mathbf{h}|$  can be approximated as*

$$F_{|\mathbf{h}|}(R_1, \dots, R_N) \approx \sum_{j_1=0}^{j_0} \sum_{j_2=0}^{j_1} \dots \sum_{j_p=0}^{j_{p-1}} \frac{g(\mathbf{s}^*)}{\pi^N \det(\mathbf{J})} \prod_{t=1}^T \frac{(-K_t)^{s_t^*}}{s_t^*! \det(\mathbf{J})^{s_t^*}} \times \prod_{n=1}^N \left( \frac{K_{n,n}}{\det(\mathbf{J})} \right)^{-\frac{\bar{s}_n}{2}-1} \left[ \Gamma \left( 1 + \frac{\bar{s}_n}{2} \right) - \Gamma \left( 1 + \frac{\bar{s}_n}{2}, \frac{K_{n,n} R_n^2}{\det(\mathbf{J})} \right) \right]. \quad (12)$$

*Proof:* See Appendix B. ■

In (12),  $\bar{s}_n$  is the sum of  $s_{t \rightarrow m, n}^*$  affecting  $|h_n|$  and

$$g(\mathbf{s}^*) = \left(\frac{1}{2}\right)^{\sum_{t=1}^T s_t^*} \sum_{\mathbf{v} \in \mathcal{V}} \left[ \prod_{t=1}^T \begin{pmatrix} s_t^* \\ v_t \end{pmatrix} \right] (2\pi)^N \prod_{i=1}^N \mathbf{1}_{\{\Delta_i=0\}}. \quad (13)$$

The expressions in (10) and (12) are extremely complicated. Nevertheless, they enable us to obtain more insightful derivations as shown later in this paper. Using the above lemmas, we present the following theorems.

**Theorem 3.** *The outage probability of FAS can be approximated in a closed-form expression as*

$$\begin{aligned} \mathbb{P}\{|h_{FAS}| < \Omega\} &= F_{|h|}(\Omega, \dots, \Omega) \\ &\approx \sum_{j_1=0}^{j_0} \sum_{j_2=0}^{j_1} \dots \sum_{j_p=0}^{j_{p-1}} \frac{g(\mathbf{s}^*)}{\pi^N \det(\mathbf{J})} \prod_{t=1}^T \frac{(-K_t)^{s_t^*}}{s_t^! \det(\mathbf{J})^{s_t^*}} \times \\ &\quad \prod_{n=1}^N \left( \frac{K_{n,n}}{\det(\mathbf{J})} \right)^{-\frac{\bar{s}_n}{2}-1} \left[ \Gamma\left(1 + \frac{\bar{s}_n}{2}\right) - \Gamma\left(1 + \frac{\bar{s}_n}{2}, \frac{K_{n,n}\Omega^2}{\det(\mathbf{J})}\right) \right]. \end{aligned} \quad (14)$$

*Proof:* The result can be obtained using Lemma 2 and substituting  $R_1 = \dots = R_N = \Omega$ . ■

*Remark 4.* According to [8],  $\mathbf{h}$  can be modeled using  $\hat{\mathbf{h}} = [\hat{h}_1, \dots, \hat{h}_N]^T$  and using the latter model, they show that the outage probability of FAS can be approximated by

$$F_{|h_{FAS}|}(\Omega) \approx \left[ \prod_{n=1}^N \int_0^\infty \frac{1}{\sum_{m=1}^{\epsilon-rank} u_{n,m}^2 \lambda_m} \exp\left(-\frac{r}{\sum_{m=1}^{\epsilon-rank} u_{n,m}^2 \lambda_m}\right) \times \left(1 - Q_1\left(\frac{\sqrt{2r}}{\Psi}, \frac{\sqrt{2}\Omega}{\Psi}\right)\right)^L dr \right]^{\frac{1}{L}}, \quad (15)$$

where  $Q_1(\cdot, \cdot)$  is the Marcum-Q function and  $L = \min\left\{\frac{1.52(N-1)}{2\pi W}, N\right\}$ . Note that (15) is a remarkable expression as each  $n$  term only has a single integral. Nevertheless, we found that it is challenging to obtain deeper insights from this expression.

**Theorem 5.** *The outage probability of FAS at high SNR is given by*

$$\mathbb{P}\{|h_{FAS}| < \Omega\} = \frac{1}{\det(\mathbf{J})} \Omega^N + o\left(\frac{1}{SNR^N}\right). \quad (16)$$

*Proof:* See Appendix C. ■



**Theorem 6.** *The diversity gain of FAS is approximately expressed as*

$$D_{\text{FAS}} \approx \min \{N, N'\}, \quad (17)$$

where  $N'$  is the rank of  $\mathbf{J}'$  such that  $\mathbf{J}'$  is the covariance matrix as defined in (2) with  $N \rightarrow \infty$  for a fixed  $W$ .

*Proof:* See Appendix D. ■

In Theorem 5, we can interpret  $\det(\mathbf{J}^{-1})$  as the penalty term and  $\Omega$  as gain of FAS that scales exponentially w.r.t.  $N$ . Meanwhile, the term with little-o can be ignored as it approaches zero if the SNR is high. Nevertheless, in Theorem 6, we can see that the diversity gain is limited by  $\min \{N, N'\}$ . Thus, increasing  $N$  over  $N'$  might not be useful. Notice that these interpretations cannot be directly obtained from (15).

#### IV. SUBOPTIMAL SOLUTION: FAS WITH $N^*$ PORTS

At a fundamental level, [9] showed that increasing the number of channels (or ports) would yield a diminishing gain (i.e., the average received SNR gain is  $\sum_n^N \frac{1}{n}$ ). In fact, [8] showed that for a fixed  $W$ , the outage probability of FAS might remain similar after some  $N$ . For ease of expositions, we denote this  $N$  as  $N^*$  where  $N^* \leq N$ .

To the best of our knowledge, little is known about  $N^*$ . In fact, it is very challenging to obtain  $N^*$  as it varies with the parameter  $W$  or more precisely the correlation matrix  $\mathbf{J}$ .<sup>4</sup> Yet, finding  $N^*$  is essential in both theory and practice since it helps FAS to achieve an efficient performance with a minimal number of ports. In this section, we present a simple method to approximate  $N^*$  for a given  $W$ .

To begin with, we present the following theorem.

**Theorem 7.** *Suppose the channels of FAS with  $N$  ports are denoted by  $\mathbf{h}$ . Then  $\mathbf{h}$  can be well-approximated by  $\tilde{\mathbf{h}} = [\tilde{h}_1, \dots, \tilde{h}_N]^T$  where*

$$\tilde{h}_n = \sum_{m=1}^{\tilde{N}} u_{n,m} \sqrt{\lambda_m} z_m, \quad (18)$$

where  $\tilde{N}$  is the numerical rank of  $\mathbf{J}$ . That is, the PDF and CDF of  $\mathbf{h}$  and  $\tilde{\mathbf{h}}$  are similar.

<sup>4</sup>Referring to (1) and (2), we can see that  $N^*$  depends on the parameter  $W$ .

*Proof:* Let  $\tilde{N}$  be the numerical rank of  $\mathbf{J}$  where  $\tilde{N} \leq N$ . Using the definition of numerical rank, we have  $\lambda_n < \epsilon$  for  $n \in \{\tilde{N} + 1, \dots, N\}$  where  $\epsilon \approx 0$ . According to Eckart-Young-Mirsky theorem [36], the optimal  $\tilde{\mathbf{J}}$  that minimizes the Frobenius norm between matrix  $\mathbf{J}$  and  $\tilde{\mathbf{J}}$  subject to the constraint that  $\text{rank}(\tilde{\mathbf{J}}) \leq \tilde{N}$  is  $\tilde{\mathbf{J}} = \mathbf{U}\tilde{\Lambda}\mathbf{U}^H$  where  $\tilde{\Lambda} = \text{diag}(\lambda_1, \dots, \lambda_{\tilde{N}}, 0, \dots, 0)$ .

Using this insight, we introduce  $\tilde{\mathbf{h}}$  as defined in Theorem 7 where the covariance of  $\tilde{\mathbf{h}}$  is  $\tilde{\mathbf{J}}$  (i.e., the best approximation of  $\mathbf{J}$  for  $\text{rank}(\tilde{\mathbf{J}}) \leq \tilde{N}$ ). As a result, we can well-approximate  $\mathbf{h}$  using  $\tilde{\mathbf{h}}$  since the Frechet distance between the two distributions is [37]

$$W_2\left(\mathcal{CN}(0_{N \times 1}, \mathbf{J}), \mathcal{CN}(0_{N \times 1}, \tilde{\mathbf{J}})\right) = \left\| (\Lambda)^{\frac{1}{2}} - (\tilde{\Lambda})^{\frac{1}{2}} \right\|_F^2 \approx 0. \quad (19)$$

■

**Corollary 8.** *If we have the exact eigenvalues and rank of  $\mathbf{J}$ , then  $\mathbf{h} = \tilde{\mathbf{h}}$ .*

*Proof:* Let  $\Lambda$  and  $\tilde{N}$  be the exact rank and eigenvalues of  $\mathbf{J}$ . Using the definition of rank, we have  $\lambda_n = 0$  for  $n \in \{\tilde{N} + 1, \dots, N\}$ . It then follows that the Frechet distance between the distributions of  $\mathbf{h}$  and  $\tilde{\mathbf{h}}$  is zero. ■

As seen in (19), it is the eigenvalues of correlation matrix that plays a critical role in the channel approximation. Motivated by this insight, we introduce a new formula as follows:

$$\varepsilon_{N^*} = S_N - S_{N^*} = \sigma^2 - S_{N^*}, \quad (20)$$

where  $S_{N^*} = \frac{1}{N} \sum_{n=1}^{N^*} \lambda_n$ . Note that (20) is analogous to (19) in the sense that the left hand side of (20) measures the gap between the distributions of  $\mathbf{h}$  and  $\mathbf{h}^*$ , where  $\mathbf{h}^*$  is similarly defined as in (18) but we instead replace  $\tilde{N}$  with  $N^*$  and impose that  $N^* \leq \tilde{N}$ . Meanwhile, on the right hand side of (20), we consider the average eigenvalues of  $\mathbf{J}^*$ , where  $\mathbf{J}^*$  is the covariance of  $\mathbf{h}^*$ .

To reduce the number of required ports, we define  $\varepsilon_{\text{tol}} > 0$  and find the smallest integer  $N^*$  such that  $\varepsilon_{\text{tol}} \geq \varepsilon_{N^*}$ . Since  $\mathbf{J}^*$  only has  $N^*$  dominant eigenvalues, we propose to employ a suboptimal FAS with  $N^*$  ports. Interestingly,  $\varepsilon_{\text{tol}}$  has a nice heuristic interpretation in practice. Specifically, it defines the sub-optimality of the proposed FAS, i.e., the proposed FAS is near optimal if  $\varepsilon_{\text{tol}}$  is small and less optimal if  $\varepsilon_{\text{tol}}$  is large.

By fixing  $\varepsilon_{\text{tol}}$  appropriately,<sup>5</sup> we observe that FAS with  $N^*$  ports yields considerable improvement over all FAS with  $N < N^*$  ports while most of the FAS with  $N > N^*$  ports yields

<sup>5</sup>We recommend to set  $\varepsilon_{\text{tol}} = 0.01\sigma^2$  (i.e., the average eigenvalues of  $\mathbf{J}^*$  is 99% of that of  $\mathbf{J}$ )

---

**Algorithm 1** Method of approximating  $N^*$  given  $W$ 


---

- 1: **Input:**  $W, \varepsilon_{\text{tol}}$ ; **Output:**  $N^*$
  - 2: Compute  $\mathbf{J} = \mathbf{U}\mathbf{\Lambda}\mathbf{U}^H$
  - 3: Define  $n = 1$  and compute  $\varepsilon_n$
  - 4: **While**  $\varepsilon_{\text{tol}} < \varepsilon_n$  and  $n < \tilde{N}$
  - 5:      $n = n + 1$
  - 6:      $\varepsilon_n = \sigma^2 - S_n$
  - 7: **end**
  - 8: **Return**  $n$  as  $N^*$
- 

marginal improvement over FAS with  $N - 1$  ports. Note that we usually have  $N^* < \tilde{N}$  if  $\mathbf{J}$  is ill-conditioned and  $N^* = \tilde{N}$  if  $\mathbf{J}$  is well-conditioned.

The method of approximating  $N^*$  is given in Algorithm 1. To measure the computational complexity of our algorithm, we consider the floating-point operations (flops). A flop is defined as one addition, subtraction, multiplication or division of two floating point numbers [38]. In Algorithm 1, computing  $\mathbf{J}$  and  $\mathbf{U}\mathbf{\Lambda}\mathbf{U}^H$  requires  $6N^2$  and  $21N^3$  flops, respectively [39]. Computing  $\varepsilon_n$  requires  $n + 1$  flops for each  $n$ . Therefore, the total flops of Algorithm 1 is  $21N^3 + 6N^2 + \frac{1}{2}N^{*2} + \frac{3}{2}N^*$ , which has a polynomial time-complexity of  $\mathcal{O}(N^3)$  since  $N^* \leq N$ . In other words, Algorithm 1 is only dominated by the computation of  $\mathbf{U}\mathbf{\Lambda}\mathbf{U}^H$ .

Note that  $N^*$  is also useful in theory. For example, Lemma 1 and 2 and Theorem 3, 5, and 6 are in calculable if  $\mathbf{J}$  is near-singular. To address this, we present the following theorem.

**Theorem 9.** *If  $\mathbf{J}$  is near-singular, then we can approximate the channels of FAS with  $N$  ports using  $N^*$  ports from a computational perspective. Nevertheless, a small gap between the channel distributions of FAS with  $N$  ports and that of  $N^*$  ports might exist.*

*Proof:* If  $\mathbf{J}$  is near-singular, then one or more entries are almost linear combinations of the other entries. Thus, we can remove these nearly-dependent entries and only consider  $N^*$  independent entries. Since FAS with  $N^*$  ports has  $N^*$  dominant eigenvalues, Lemma 1 and 2 and Theorem 3, 5, and 6 are calculable. Nevertheless, there might be a small gap between the channel distributions of FAS with  $N$  ports and that of  $N^*$  ports since the entries are nearly-dependent only. ■

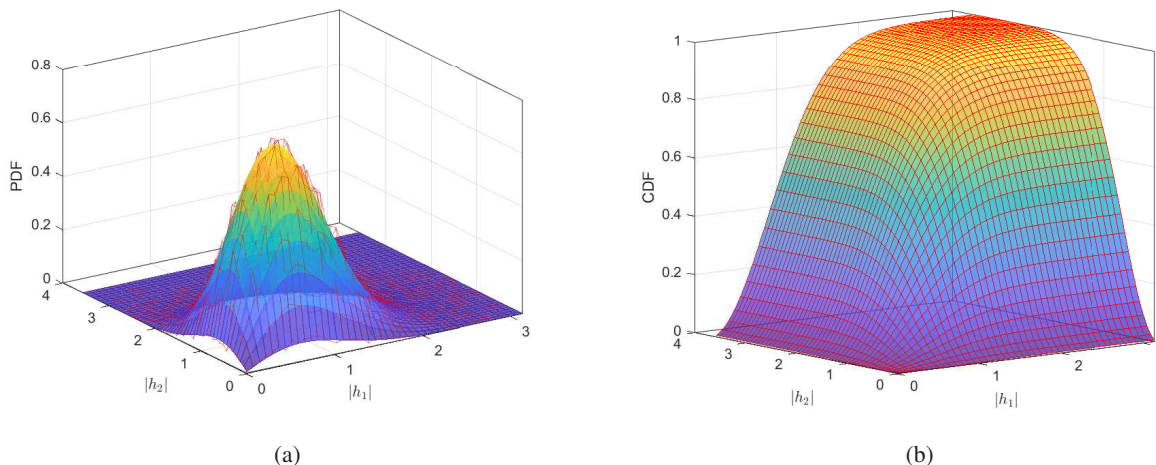


Figure 1: FAS with 2 ports: (a) joint PDF; (b) joint CDF.

## V. RESULTS AND DISCUSSION

In this section, we present simulation results to better understand the performance of FAS. We focus on the design of an efficient FAS as well as the factors that limit its performance. Unless stated otherwise, we assume that  $\sigma^2 = 1$ ,  $N = 50$ ,  $W = 0.5$ ,  $q = 10$  and  $SNR = 30\text{dB}$ .

Firstly, we demonstrate the accuracy of (10) and (12). In order to visualize the joint PDF and CDF of  $|\mathbf{h}|$ , we consider a FAS with 2 ports (i.e.,  $N = 2$ ). In Fig. 1, the red grid represents the numerical PDF/CDF while the solid surface is the analytical PDF/CDF. As observed, the approximation of the PDF/CDF of  $|\mathbf{h}|$  matches closely with the numerical ones over all the distributed region. Still, it is worth noting that (10) and (12) are very complicated. Thus, approximations with simpler expressions remain desirable.

In Fig. 2, we compute the outage probability of FAS versus SNR for different  $N$  and  $W$ . Comparing Fig. 2(a) and Fig. 2(b), we can clearly see that the outage probability is mainly limited by  $W$ . In particular, if  $W$  is small and  $N$  is large, the outage probability remains similar which is in alignment with the findings of [8]. Nevertheless, if  $W$  is sufficiently large, the outage probability decreases significantly as  $N$  increases.

To better understand this, we further compare the outage probability of FAS to (15) and (16). In Fig. 3, we can see that (15) is less accurate while (16) is accurate as  $SNR$  increases. From (16), we learn that  $\det(\mathbf{J}^{-1})$  plays a critical role in the performance of FAS. In particular,  $\mathbf{J}$  has to be well-conditioned in order for  $\Omega^N$  to be the dominant term. If  $\mathbf{J}$  is near-singular, then

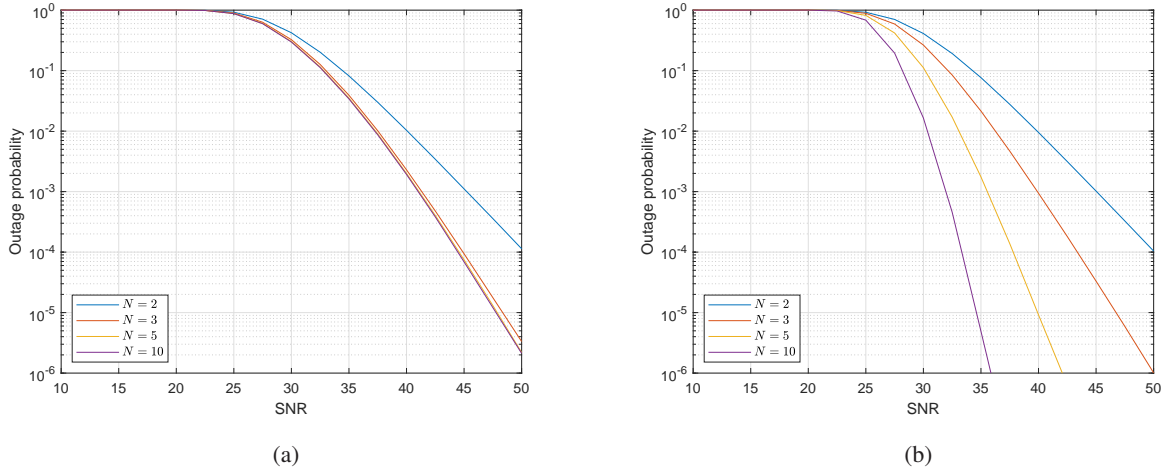


Figure 2: Outage probability of FAS versus SNR for different  $N$  and  $W$ : (a)  $W = 0.5$ ; (b)  $W = 10$ .

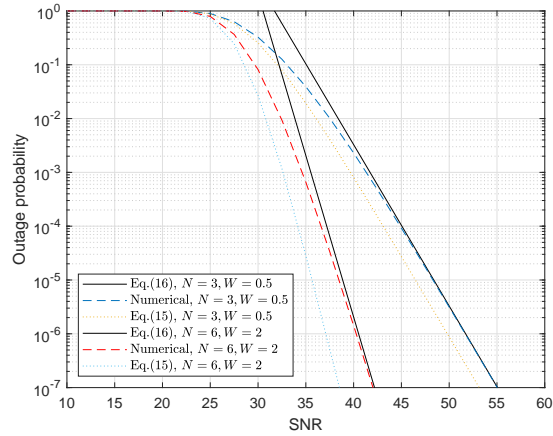


Figure 3: Outage probability of FAS at high SNR.

the parameter  $N$  is no longer important. This is because  $\det(\mathbf{J}^{-1})$  cannot be compensated by  $\Omega^N$ . To make  $\mathbf{J}$  a well-conditioned matrix, we can either increase  $W$  for a fixed  $N$  or decrease  $N$  for a fixed  $W$ . Nevertheless, we believe that larger  $N$  does not cause any harm to the system in practice. It only makes the theoretical analysis harder.

As shown in Fig. 4(a), we compare the outage probability of FAS with  $N$  ports and that of  $N'$  ports for different  $W$  where  $N < N'$ . As it is seen, the outage probability of the earlier is lower bounded by the latter regardless of  $W$ . In Fig. 4(b), we investigate the opposite case

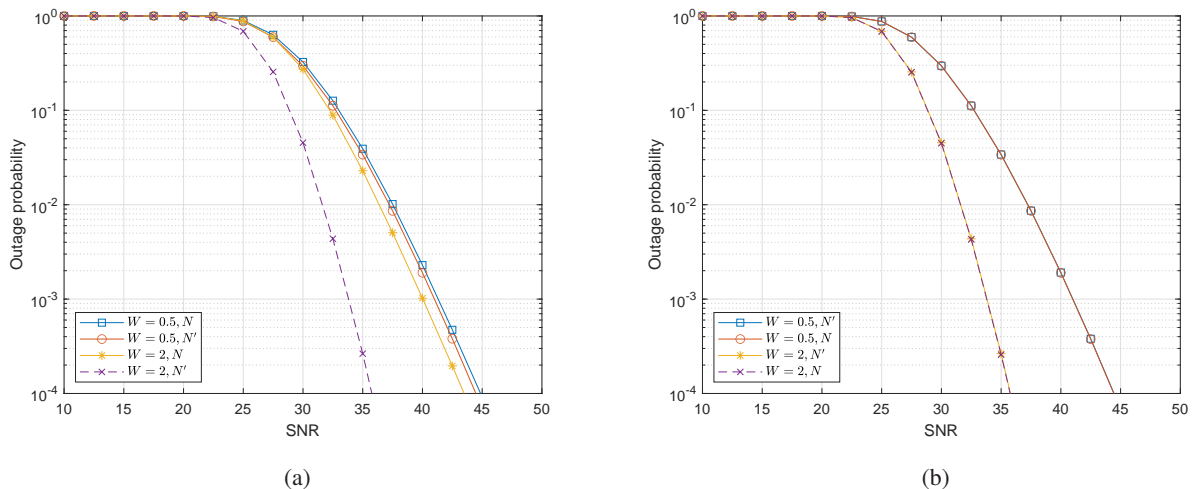


Figure 4: Outage probability of FAS with  $N$  ports versus  $\tilde{N}$  ports: (a)  $N = 3 < \tilde{N}$ ; (b)  $N = 50 > \tilde{N}$ .

where  $N > N'$ . As observed, the outage probability of FAS with  $N$  ports and that of  $N'$  ports are the same for different  $W$ . Thus, the diversity gain of FAS is limited by  $\min\{N, N'\}$ , which verifies Theorem 6. Theorem 6 also suggests that increasing the ports beyond  $N'$  provides no improvement in a point-to-point setting.

Fig. 5(a) presents the CDF of  $\mathbf{h}$  and  $\tilde{\mathbf{h}}$  where we fix  $R_1 = \dots = R_N = R$ . In the result, no significant variation is observed between  $\mathbf{h}$  and  $\tilde{\mathbf{h}}$  regardless of  $R$ ,  $N$  and  $W$ . This is because the Fréchet distance between the two distributions is always near zero. This confirms Theorem 7 and suggests that one can always use  $\tilde{\mathbf{h}}$  instead of  $\mathbf{h}$ . In addition, Fig. 5(b) shows the CDF of  $\mathbf{h}$  and  $\mathbf{h}^*$ . Unlike the previous result, there is a small gap between the two distributions as  $W$  increases. Despite having some gaps, the approximation is still fairly good. This result verifies Theorem 9.

Next, we investigate the accuracy of Algorithm 1 and the efficiency of the proposed suboptimal FAS. The parameter  $N^*$  for different  $W$  using Algorithm 1 is summarized in Table I. As it is seen, the outage probability of FAS with  $N^*$  ports is promising. Specifically, FAS with  $N^*$  ports yields a significant improvement over FAS with  $N^* - 1$  ports. Meanwhile, FAS with  $N + 1$  ports provides negligible improvement over FAS with  $N^*$  ports. Thus, we may use the suboptimal FAS for an efficient performance.

Finally in Fig. 7, we compare the outage probability of the proposed suboptimal FAS, the

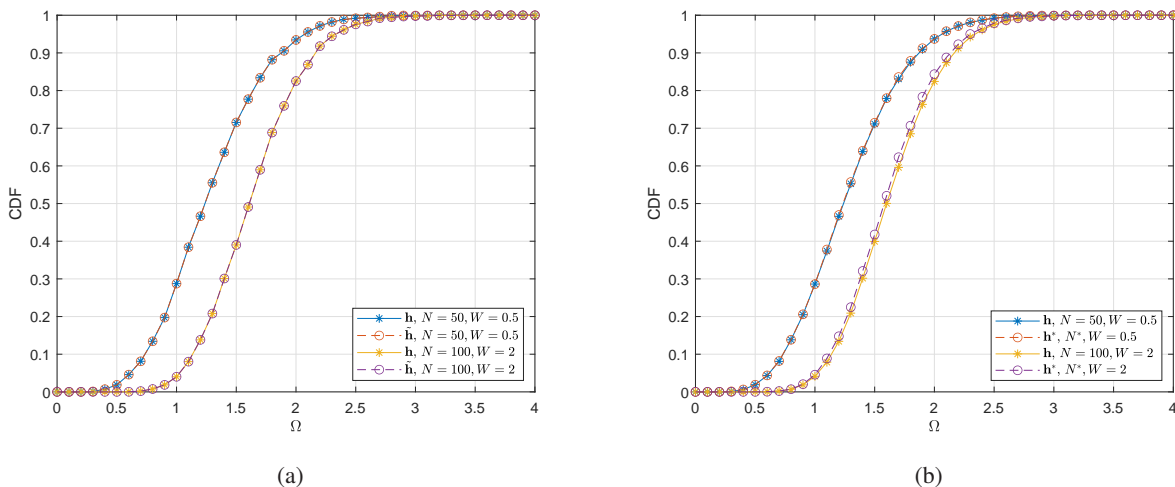


Figure 5: CDF between: (a)  $h$  and  $\tilde{h}$ ; (b)  $h$  and  $h^*$ .

Table I: Parameter  $N^*$  generated by algorithm 1 for different  $W$ .

$W$	0.5	1	2	3	4
$N^*$	3	4	6	8	10

optimal FAS, the single antenna (SISO) system, the  $N$ -branch SC system, and the  $N$ -branch MRC system. In SC and MRC systems, we assume there are  $N$  RF-chains where each antenna has to be at least  $\frac{\lambda}{2}$  apart and their spatial correlations are considered. Results show that the proposed suboptimal FAS outperforms SISO and SC systems. This improvement is due to the ability of FAS switching to the best port within a finite  $W$ .

In addition, MRC has the lowest outage probability. It outperforms optimal FAS. This superiority is due to the power gain where a larger number of active RF-chains (i.e.,  $\lfloor \frac{W}{0.5} \rfloor + 1$ ) is utilized. Although MRC is more superior than the suboptimal FAS, the latter can achieve a similar performance as compared to the earlier when  $W = 0.5$ . Yet, it is important to recall that MRC has one additional RF-chain as compared to the suboptimal FAS in this case. Thus, it will be very interesting to compare the performance of MIMO-FAS and MIMO with the same number of RF-chains.

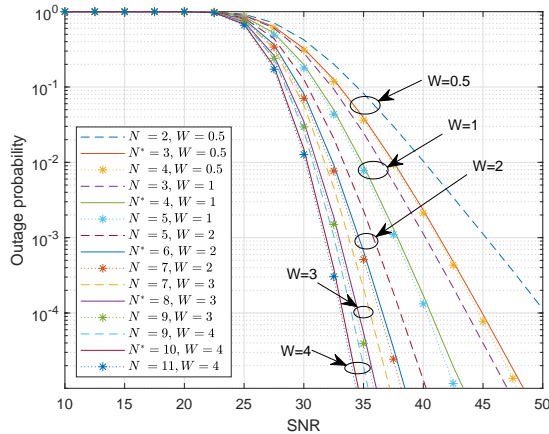


Figure 6: Outage probability of suboptimal FAS.

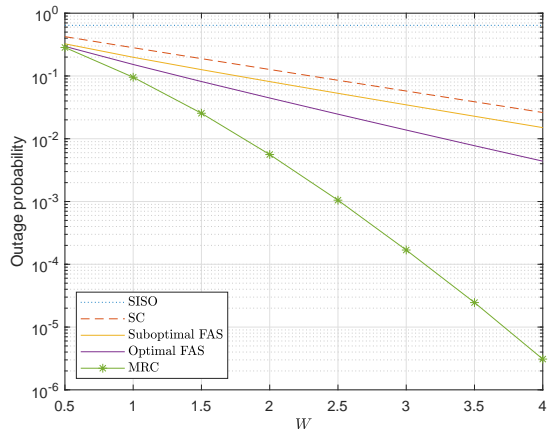


Figure 7: Outage probability of suboptimal FAS vs. SISO, SC, and MRC.

## VI. CONCLUSIONS

In this paper, we consider FAS and approximate its outage probability and diversity gain in closed-form expressions. New meaningful insights are obtained from the analytical results, and simulation results are given to better understand the factors that limit the performance of FAS. Our results show that the performance of FAS strongly depends on the spatial correlation matrix  $\mathbf{J}$ . Specifically, increasing the ports beyond  $N'$  yields no diversity gain in a point-to-point setting. Instead, increasing  $N$  causes the correlation matrix  $\mathbf{J}$  to be ill-conditioned. To address this, one can either increase  $W$  for a fixed  $N$  or decrease  $N$  for a fixed  $W$ . In addition, we propose a suboptimal FAS with  $N^*$  ports. By fixing an appropriate  $\varepsilon_{\text{tol}}$ , the proposed scheme enables us to



obtain a significant gain over FAS with  $N^* - 1$  while it nearly achieves the same performance as FAS with  $N^* + 1$  ports. Thus, the approximation of  $N^*$  is pragmatically useful since a larger number of ports yields diminishing gains and additional costs. Furthermore,  $N^*$  can be used to approximate the channels of FAS with  $N$  ports if the correlation matrix  $\mathbf{J}$  is near-singular. Last but not least, the proposed suboptimal FAS outperforms SISO and SC systems but falls behind MRC due to having a single active RF-chain. Nevertheless, it is discovered that suboptimal FAS and MRC achieve similar performance when  $W = 0.5$ . Thus, it will be interesting to study the performance of MIMO-FAS and MIMO in the future.

#### APPENDIX A: APPROXIMATED PDF OF $|\mathbf{h}|$

The exact PDF of  $|\mathbf{h}|$  is first derived in [23]–[25]. In this paper, we employ similar steps and further approximate the PDF of  $|\mathbf{h}|$  by introducing  $\mathbf{G}$ : an  $N \times N$  matrix, using an accurate binomial theorem, and truncating the infinite series to a finite one for ease of computation. According to [34], the PDF of a circularly symmetric complex Gaussian random variables is known as

$$f(\mathbf{h}) = \frac{1}{\pi^N \det(\mathbf{J})} \exp\{-\mathbf{h}^H \mathbf{J}^{-1} \mathbf{h}\}, \quad (21)$$

where  $\mathbf{J}^{-1} = \frac{\mathbf{K}^T}{\det(\mathbf{J})}$  via Crammer rule. Using [40, (7-8) & (7-9)], the PDF of (21) in terms of its amplitude and phase can be obtained as

$$f_{|\mathbf{h}|, \boldsymbol{\theta}}(|h_1|, \theta_1, \dots, |h_N|, \theta_N) = \eta \prod_{t=1}^T \exp\{\zeta_t \cos(\bar{\theta}_t)\}, \quad (22)$$

where  $\eta = \frac{\prod_{n=1}^N |h_n|}{\pi^N \det(\mathbf{J})} \exp\left\{-\frac{\sum_{n=1}^N |h_n|^2 K_{n,n}}{\det(\mathbf{J})}\right\}$ ,  $T = \frac{N(N-1)}{2}$ ,  $\zeta_t = -\frac{2K_{m,n}|h_n||h_m|}{\det(\mathbf{J})}$  and  $\bar{\theta}_t = \theta_n - \theta_m$ . In (22), we use the mapping function where  $t = n + (m-1)N - \frac{m(m+1)}{2}$ ,  $m < n$ , while  $(m, n)$  can be obtained from  $t$  by setting  $m = \min m' \in \mathbb{Z}$  subject to  $\sum_{i=1}^{m'} (N-i) > t$  and  $n = t - (m-1)N + \frac{m(m+1)}{2}$ .

Integrating (22) w.r.t.  $\theta_n, \forall n$  over  $[0, 2\pi]$ , we have

$$\begin{aligned} & f_{|\mathbf{h}|}(|h_1|, \dots, |h_N|) \\ &= \int_0^{2\pi} \cdots \int_0^{2\pi} f(|h_1|, \theta_1, \dots, |h_N|, \theta_N) d\theta_1 \dots d\theta_N \end{aligned} \quad (23)$$

$$\stackrel{(a)}{=} \eta \int_0^{2\pi} \cdots \int_0^{2\pi} \prod_{t=1}^T \sum_{s_t=0}^{\infty} \frac{\zeta_t^{s_t}}{s_t!} \cos(\bar{\theta}_t)^{s_t} d\theta_1 \dots d\theta_N \quad (24)$$

$$\stackrel{(b)}{=} \eta \sum_{s_1=0}^{\infty} \sum_{s_2=0}^{s_1} \cdots \sum_{s_{T-1}=0}^{s_{T-2}} \prod_{t=1}^T \beta(t, s_t^*) \int_0^{2\pi} \cdots \int_0^{2\pi} \cos(\bar{\theta}_t)^{s_t^*} d\theta_1 \dots d\theta_N \quad (25)$$

$$\stackrel{(c)}{=} \eta \sum_{s_1=0}^{\infty} \sum_{s_2=0}^{s_1} \cdots \sum_{s_{T-1}=0}^{s_{T-2}} \left(\frac{1}{2}\right)^{\sum_{t=1}^T s_t^*} \prod_{t=1}^T \beta(t, s_t^*) \times \quad (26)$$

$$\int_0^{2\pi} \cdots \int_0^{2\pi} \prod_{t=1}^T (\exp\{j\bar{\theta}_t\} + \exp\{-j\bar{\theta}_t\})^{s_t^*} d\theta_1 \dots d\theta_N$$

$$\stackrel{(d)}{=} \eta \sum_{s_1=0}^{\infty} \cdots \sum_{s_{T-1}=0}^{s_{T-2}} \left(\frac{1}{2}\right)^{\sum_{t=1}^T s_t^*} \prod_{t=1}^T \beta(t, s_t^*) \sum_{\mathbf{v} \in \mathcal{V}} \prod_{t=1}^T \binom{s_t^*}{v_t} \times \quad (27)$$

$$\int_0^{2\pi} \cdots \int_0^{2\pi} \exp\left\{j \sum_{t=1}^T \gamma_t \bar{\theta}_t\right\} d\theta_1 \dots d\theta_N,$$

where (24) is obtained by using  $\exp\{x\} = \sum_{s=0}^{\infty} \frac{x^s}{s!}$  and (25) is obtained using Cauchy product of power series where  $\beta(t, s_t) \triangleq \frac{\zeta_t^{s_t}}{s_t!}$  and  $s_t^* = s_t - s_{t+1}$  with  $s_{T+1} = 0$ . Furthermore, (26) is obtained using  $\cos(x) = \frac{\exp(jx) + \exp(-jx)}{2}$  and (27) is obtained using binomial theorem where  $\mathbf{v} = [v_1, \dots, v_T]^T$ ,  $\mathcal{V}$  denotes the set of all the possible permutations and  $\gamma_t = 2v_t - j_t^* \in \mathbb{Z}$ .

Note that  $\int_0^{2\pi} \cdots \int_0^{2\pi} \exp\left\{j \sum_{t=1}^T \gamma_t \bar{\theta}_t\right\} d\theta_1 \dots d\theta_N = (2\pi)^N$  if and only if  $\sum_{t=1}^T \gamma_t \bar{\theta}_t = 0$ , and otherwise zero. Therefore, we introduce a new matrix  $\mathbf{G}$  as defined in (11) and the matrix  $\bar{\Theta}$  given by

$$\bar{\Theta} = \begin{bmatrix} 0 & \bar{\theta}_1 & \bar{\theta}_2 & \cdots & \bar{\theta}_{N-1} \\ & & \bar{\theta}_N & \cdots & \bar{\theta}_{2N-3} \\ \vdots & \ddots & & \vdots & \\ & & & \bar{\theta}_T & \\ 0 & \cdots & 0 & & \end{bmatrix} = \begin{bmatrix} 0 & \theta_2 - \theta_1 & \theta_3 - \theta_1 & \cdots & \theta_N - \theta_1 \\ & & \theta_3 - \theta_2 & \cdots & \theta_N - \theta_2 \\ \vdots & & \ddots & & \vdots \\ & & & & \theta_N - \theta_{N-1} \\ 0 & \cdots & & & 0 \end{bmatrix}. \quad (28)$$

Using  $\bar{\Theta}$  and  $\mathbf{G}$ , we can easily integrate (27) w.r.t. to  $\theta_i$  by taking the sum of the same entries

of  $\mathbf{G}$  as that of  $\bar{\Theta}$  with  $\theta_i$ , i.e.,  $\Delta_i = \sum_{n=1}^N G_{i,n} + \sum_{n=1}^N G_{n,i} - G_{i,i}$ . Therefore, (27) leads to

$$(27) = \eta \sum_{s_1=0}^{\infty} \sum_{s_2=0}^{s_1} \cdots \sum_{s_T=0}^{s_{T-1}} \left(\frac{1}{2}\right)^{\sum_{t=1}^T s_t^*} \prod_{t=1}^T \beta(t, s_t^*) \sum_{\mathbf{v} \in \mathcal{V}} \left[ \prod_{t=1}^T \binom{s_t^*}{v_t} \right] \left[ (2\pi)^N \prod_{i=1}^N \mathbf{1}_{\{\Delta_i=0\}} \right] \quad (29)$$

$$\stackrel{(a)}{\approx} \eta \sum_{s_1=0}^{s_0} \sum_{s_2=0}^{s_1} \cdots \sum_{s_T=0}^{s_{T-1}} \left(\frac{1}{2}\right)^{\sum_{t=1}^T s_t^*} \prod_{t=1}^T \beta(t, s_t^*) \sum_{\mathbf{v} \in \mathcal{V}} \left[ \prod_{t=1}^T \binom{s_t^*}{v_t} \right] \left[ (2\pi)^N \prod_{i=1}^N \mathbf{1}_{\{\Delta_i=0\}} \right], \quad (30)$$

where (a) can be obtained since  $\beta(t, s_t^*) \approx 0$  if  $s_t^*$  is sufficiently large.

## APPENDIX B: APPROXIMATED CDF OF $|\mathbf{h}|$

Using (10), the CDF of  $|\mathbf{h}|$  can be obtained as

$$F(R_1, \dots, R_N) \approx \int_0^{R_1} \cdots \int_0^{R_N} f_{|\mathbf{h}|}(|h_1|, \dots, |h_N|) d|h_1| \cdots d|h_N| \quad (31)$$

$$= \sum_{s_1=0}^{s_0} \sum_{s_2=0}^{s_1} \cdots \sum_{s_T=0}^{s_{T-1}} \frac{g(\mathbf{s}^*)}{\pi^N \det(\mathbf{J})} \prod_{t=1}^T \frac{(-2K_{m,n \rightarrow t})^{s_t^*}}{s_t^! \det(\mathbf{J})^{s_t^*}} \int_0^{R_1} \cdots \int_0^{R_N} \times \quad (32)$$

$$\prod_{n=1}^N |h_n| \prod_{n=1}^N \prod_{m < n} (|h_n| |h_m|)^{s_{t \rightarrow m, n}^*} \exp \left\{ -\frac{\sum_{n=1}^N |h_n|^2 K_{n,n}}{\det(\mathbf{J})} \right\} d|h_1| \cdots d|h_N|$$

$$= \sum_{s_1=0}^{s_0} \sum_{s_2=0}^{s_1} \cdots \sum_{s_T=0}^{s_{T-1}} \frac{g(\mathbf{s}^*)}{\pi^N \det(\mathbf{J})} \prod_{t=1}^T \frac{(-2K_{m,n \rightarrow t})^{s_t^*}}{s_t^! \det(\mathbf{J})^{s_t^*}} \times \quad (33)$$

$$\prod_{n=1}^N \int_0^{R_n} |h_n|^{\bar{s}_n+1} \exp \left\{ -\frac{|h_n|^2 K_{n,n}}{\det(\mathbf{J})} \right\} d|h_1| \cdots d|h_N|$$

$$= \sum_{j_1=0}^{j_0} \sum_{j_2=0}^{j_1} \cdots \sum_{j_p=0}^{j_{p-1}} \frac{g(\mathbf{s}^*)}{\pi^N \det(\mathbf{J})} \prod_{t=1}^T \frac{(-K_t)^{s_t^*}}{s_t^! \det(\mathbf{J})^{s_t^*}} \times \quad (34)$$

$$\prod_{n=1}^N \left( \frac{K_{n,n}}{\det(\mathbf{J})} \right)^{-\frac{\bar{s}_n}{2}-1} \left[ \Gamma \left( 1 + \frac{\bar{s}_n}{2} \right) - \Gamma \left( 1 + \frac{\bar{s}_n}{2}, \frac{K_{n,n} R_n^2}{\det(\mathbf{J})} \right) \right],$$

where  $\bar{s}_n$  is the sum of  $s_{t \rightarrow m, n}^*$  affecting  $(|h_n| |h_m|)^{s_{t \rightarrow m, n}^*}$  and

$$g(\mathbf{s}^*) = \left(\frac{1}{2}\right)^{\sum_{t=1}^T s_t^*} \sum_{\mathbf{v} \in \mathcal{V}} \left[ \prod_{t=1}^T \binom{s_t^*}{v_t} \right] (2\pi)^N \prod_{i=1}^N \mathbf{1}_{\{\Delta_i=0\}}.$$

APPENDIX C: OUTAGE PROBABILITY OF FAS AT HIGH SNR

According to [35], the outage probability of a wireless communication system at high SNR can be obtained via the PDF of its fading channels. In particular, suppose the PDF of the channels at high SNR can be approximated as

$$f_{|h_{\text{FAS}}|}(\Omega) = 2\xi\Omega^{2M+1} + o(\Omega^{2M+1}). \quad (35)$$

Then the outage probability at high SNR is found as

$$\mathbb{P}\{|h_{\text{FAS}}| < \Omega\} = \frac{\xi}{M+1}\Omega^{M+1} + o\left(\frac{1}{\text{SNR}^{M+1}}\right). \quad (36)$$

Before approximating the PDF of FAS at high SNR, we highlight that the PDF of (21) in terms of its amplitude and phase can be rewritten as

$$f_{|h|,\boldsymbol{\theta}}(|h_1|, \theta_1, \dots, |h_N|, \theta_N) = \prod_{n=1}^N \frac{|h_n| H_n}{\pi^N \det(\mathbf{J})} \quad (37)$$

where

$$H_n = \exp\left\{-\frac{K_{n,n}|h_n|^2 + 2\sum_{m=n+1}^N K_{m,n}|h_n||h_m|\cos(\theta_n - \theta_m)}{\det(\mathbf{J})}\right\}. \quad (38)$$

Using (37), the approximated PDF of FAS at high SNR can be derived as

$$f_{|h_{\text{FAS}}|}(\Omega) = \frac{\partial F_{|h_{\text{FAS}}|}(\Omega)}{\partial \Omega} \quad (39)$$

$$\stackrel{(a)}{=} N \int_0^\Omega \dots \int_0^\Omega \int_0^{2\pi} \dots \int_0^{2\pi} f_{|h|,\boldsymbol{\theta}}(|h_1|, \theta_1, \dots, |h_{N-1}|, \theta_{N-1}, \Omega, \theta_N) \quad (40)$$

$$d|h_1| \dots d|h_{N-1}| d\theta_1 \dots d\theta_N$$

$$\stackrel{(b)}{=} \frac{N\Omega}{\pi^N \det(\mathbf{J})} \int_0^{2\pi} \dots \int_0^{2\pi} H_N \int_0^\Omega |h_{N-1}| \left( H_{N-1} \times \dots \right. \quad (41)$$

$$\left. \left( \int_0^\Omega |h_2| H_2 \left( \int_0^\Omega |h_1| H_1 d|h_1| \right) d|h_2| \right) \dots d|h_{N-1}| \right) d\theta_1 \dots d\theta_N,$$

where (a) is obtained using Leibniz integral and (b) is obtained using (37).

According to [41], the term  $\int_0^\Omega |h_n| H_n d|h_n|$  can be solved by applying Taylor series approximation at around zero. Specifically, we have

$$\int_0^\Omega |h_n| H_n d|h_n| = \frac{\Omega^2}{2} + o(\Omega^2), n = \{1, \dots, N-1\} \quad (42)$$

and the Taylor series approximation of  $H_N$  at zero is

$$H_N = 1 + o(1). \quad (43)$$

Substituting (42) and (43) into (41), we have

$$f_{|h_{\text{FAS}}|}(\Omega) = \frac{N\Omega}{\pi^N \det(\mathbf{J})} \left[ \frac{\Omega^2}{2} + o(\Omega^2) \right]^{N-1} \int_0^{2\pi} \cdots \int_0^{2\pi} d\theta_1 \cdots d\theta_N \quad (44)$$

$$= \frac{2N}{\det(\mathbf{J})} \Omega^{2N-1} + o(\Omega^{2N-1}). \quad (45)$$

Comparing (45) to (35), we have  $M = N - 1$  and  $\xi = \frac{N}{\det(\mathbf{J})}$ . Applying (36), we have

$$\mathbb{P}\{|h_{\text{FAS}}| < \Omega\} \approx \frac{\Omega^N}{\det(\mathbf{J})} + o\left(\frac{1}{\text{SNR}^N}\right). \quad (46)$$

#### APPENDIX D: DIVERSITY GAIN OF FAS

Let us consider the case where  $W \rightarrow \infty$ . According to [35], the diversity gain of a wireless communication system can be obtained via the PDF of its fading channels at high SNR. Specifically, suppose the PDF of the channels at high SNR can be approximated as in (35). Then diversity gain of such system is given by

$$D = M + 1. \quad (47)$$

In Appendix C, we have  $M = N - 1$ . Thus, it is straightforward that the diversity gain of FAS as  $W \rightarrow \infty$  is  $N$ . Nevertheless, if  $W$  is finite,  $\mathbf{J}$  might be near to being singular. To see this, let us consider FAS with  $N \rightarrow \infty$  ports within a finite  $W$  where each port is equally separated, and they are indexed as  $1, 2, \dots$ . Without loss of generality, let us focus on two ports:  $n$ -th and  $(n + 1)$ -th port. The correlation between the  $n$ -th port and  $(n + 1)$ -th port is  $\mathbf{J}_{n,n+1} = \lim_{N \rightarrow \infty} \sigma^2 J_0\left(2\pi \frac{1}{N-1} W\right) = \sigma^2 J_0(0)$ , and we have  $h_{n+1} = h_n$ . Thus, the joint CDF of  $h_n$  and  $h_{n+1}$  is  $F_{h_n, h_{n+1}}(g_1, g_2) = F_{h_n}(\min\{g_1, g_2\})$ , which implies that they reduce to singularity. Since there are many such ports, we can use a finite  $N'$  ports to approximate the channels of FAS with  $N$  ports, where  $N'$  is the rank of  $\mathbf{J}'$  such that  $\mathbf{J}'$  is covariance matrix as defined in (2) with  $N \rightarrow \infty$  for a fixed  $W$ . As a result, the diversity gain of FAS is approximately limited by  $\min\{N, N'\}$ . If  $N$  is large, the same observation can be obtained. To remove the nearly-dependent entries of  $\mathbf{J}$ , one may employ rank-revealing QR factorization [42] or Gauss-Jordan elimination with a given tolerance.

#### REFERENCES

- [1] A. Shojaeifard, K.-K. Wong, K.-F. Tong, Z. Chu, A. Mourad, A. Haghigat, I. Hemaddeh, N. T. Nguyen, V. Tapio, and M. Juntti, "MIMO evolution beyond 5G through reconfigurable intelligent surfaces and fluid antenna systems," *Proceedings of the IEEE*, vol. 110, no. 9, pp. 1244–1265, 2022. **I**

- [2] K. K. Wong, K.-F. Tong, Y. Shen, Y. Chen, and Y. Zhang, "Bruce Lee-inspired fluid antenna system: Six research topics and the potentials for 6G," *Frontiers in Communications and Networks*, p. 5, 2022. **I**
- [3] K.-K. Wong, A. Shojaeifard, K.-F. Tong, and Y. Zhang, "Fluid antenna systems," *IEEE Transactions on Wireless Communications*, vol. 20, no. 3, pp. 1950–1962, 2021. **I, II**
- [4] E. Basar, M. Di Renzo, J. De Rosny, M. Debbah, M.-S. Alouini, and R. Zhang, "Wireless communications through reconfigurable intelligent surfaces," *IEEE Access*, vol. 7, pp. 116 753–116 773, 2019. **I**
- [5] K.-K. Wong, K.-F. Tong, Z. Chu, and Y. Zhang, "A vision to smart radio environment: Surface wave communication superhighways," *IEEE Wireless Communications*, vol. 28, no. 1, pp. 112–119, 2021. **I**
- [6] O. Elijah, S. K. Abdul Rahim, W. K. New, C. Y. Leow, K. Cumanan, and T. Kim Geok, "Intelligent massive MIMO systems for beyond 5G networks: An overview and future trends," *IEEE Access*, vol. 10, pp. 102 532–102 563, 2022. **I**
- [7] C.-X. Wang, J. Wang, S. Hu, Z. H. Jiang, J. Tao, and F. Yan, "Key technologies in 6G terahertz wireless communication systems: A survey," *IEEE Vehicular Technology Magazine*, vol. 16, no. 4, pp. 27–37, 2021. **I**
- [8] M. Khammassi, A. Kammoun, and M.-S. Alouini, "A new analytical approximation of the fluid antenna system channel," *arXiv preprint arXiv:2203.09318*, 2022. **I, II, 4, IV, V**
- [9] D. G. Brennan, "Linear diversity combining techniques," *Proceedings of the IRE*, vol. 47, no. 6, pp. 1075–1102, 1959. **I, IV**
- [10] K. K. Wong, A. Shojaeifard, K.-F. Tong, and Y. Zhang, "Performance limits of fluid antenna systems," *IEEE Communications Letters*, vol. 24, no. 11, pp. 2469–2472, 2020. **I**
- [11] K.-K. Wong and K.-F. Tong, "Fluid antenna multiple access," *IEEE Transactions on Wireless Communications*, vol. 21, no. 7, pp. 4801–4815, 2022. **I**
- [12] C. Skouroumounis and I. Krikidis, "Large-scale fluid antenna systems with linear MMSE channel estimation," in *ICC 2022 - IEEE International Conference on Communications*, 2022, pp. 1330–1335. **I**
- [13] L. Tlebaldiyeva, G. Nauryzbayev, S. Arzykulov, A. Eltawil, and T. Tsiftsis, "Enhancing QoS through fluid antenna systems over correlated Nakagami-m fading channels," in *2022 IEEE Wireless Communications and Networking Conference (WCNC)*, 2022, pp. 78–83. **I**
- [14] K. Wong, K. Tong, Y. Chen, and Y. Zhang, "Closed-form expressions for spatial correlation parameters for performance analysis of fluid antenna systems," *Electronics Letters*, vol. 58, no. 11, pp. 454–457, 2022. **I**
- [15] K. N. Le, "A review of selection combining receivers over correlated rician fading," *Digital Signal Processing*, vol. 88, pp. 1–22, 2019. [Online]. Available: <https://www.sciencedirect.com/science/article/pii/S1051200418307176> **I**
- [16] K. S. Miller, "Complex Gaussian processes," *Siam Review*, vol. 11, no. 4, pp. 544–567, 1969. **I**
- [17] C. Tan and N. Beaulieu, "Infinite series representations of the bivariate Rayleigh and Nakagami-m distributions," *IEEE Transactions on Communications*, vol. 45, no. 10, pp. 1159–1161, 1997. **I**
- [18] P. Dharmawansa, N. Rajatheva, and C. Tellambura, "On the trivariate Rician distribution," *IEEE Transactions on Communications*, vol. 56, no. 12, pp. 1993–1997, 2008. **I**
- [19] Y. Chen and C. Tellambura, "Infinite series representations of the trivariate and quadrivariate Rayleigh distribution and their applications," *IEEE Transactions on Communications*, vol. 53, no. 12, pp. 2092–2101, 2005. **I**
- [20] M. Tekinay and C. Beard, "Moments of the quadrivariate Rayleigh distribution with applications for diversity receivers," *Annals of Telecommunications*, vol. 75, no. 7, pp. 447–459, 2020. **I**
- [21] Y. Chen and C. Tellambura, "Distribution functions of selection combiner output in equally correlated Rayleigh, Rician, and Nakagami-m fading channels," *IEEE Transactions on Communications*, vol. 52, no. 11, pp. 1948–1956, 2004. **I**
- [22] G. Karagiannidis, D. Zogas, and S. Kotsopoulos, "On the multivariate Nakagami-m distribution with exponential correlation," *IEEE Transactions on Communications*, vol. 51, no. 8, pp. 1240–1244, 2003. **I**

- [23] M. Wiegand and S. Nadarajah, "A series representation for multidimensional Rayleigh distributions," *International Journal of Communication Systems*, vol. 31, no. 6, p. e3510, 2018, e3510 dac.3510. [Online]. Available: <https://onlinelibrary.wiley.com/doi/abs/10.1002/dac.3510> **I, VI**
- [24] —, "Series approximations for Rayleigh distributions of arbitrary dimensions and covariance matrices," *Signal Processing*, vol. 165, pp. 20–29, 2019. **I, VI**
- [25] —, "New generalised approximation methods for the cumulative distribution function of arbitrary multivariate Rayleigh random variables," *Signal Processing*, vol. 176, p. 107664, 2020. [Online]. Available: <https://www.sciencedirect.com/science/article/pii/S0165168420302073> **I, VI**
- [26] R. G. Gallager, *Principles of digital communication*. Cambridge University Press Cambridge, UK, 2008, vol. 1. **2**
- [27] Z. Chai, K.-K. Wong, K.-F. Tong, Y. Chen, and Y. Zhang, "Port selection for fluid antenna systems," *IEEE Communications Letters*, vol. 26, no. 5, pp. 1180–1184, 2022. **I**
- [28] L. Zhu, W. Ma, and R. Zhang, "Modeling and performance analysis for movable antenna enabled wireless communications," *arXiv preprint arXiv:2210.05325*, 2022. **I**
- [29] W. Ma, L. Zhu, and R. Zhang, "MIMO capacity characterization for movable antenna systems," *arXiv preprint arXiv:2210.05396*, 2022. **I**
- [30] N. Waqar, K.-K. Wong, K.-F. Tong, and S. Adrian, "Deep learning enabled slow fluid antenna multiple access," *Submitted to IEEE Communications Letters*, 2022. **I, 3**
- [31] K.-K. Wong, K.-F. Tong, Y. Chen, and Y. Zhang, "Fast fluid antenna multiple access enabling massive connectivity," *Submitted to IEEE Communications Letters*, 2022. **I**
- [32] H. Xu, K.-K. Wong, W. K. New, and K.-F. Tong, "On the outage probability for two-user fluid antenna multiple access," *Submitted to 2023 IEEE International Conference on Communications (ICC)*, 2023. **I**
- [33] G. L. Stüber and G. L. Steuber, *Principles of mobile communication*. Springer, 1996, vol. 2. **II**
- [34] D. Tse and P. Viswanath, *Fundamentals of wireless communication*. Cambridge university press, 2005. **II, VI**
- [35] Z. Wang and G. Giannakis, "A simple and general parameterization quantifying performance in fading channels," *IEEE Transactions on Communications*, vol. 51, no. 8, pp. 1389–1398, 2003. **II, VI, VI**
- [36] G. Golub, A. Hoffman, and G. Stewart, "A generalization of the eckart-young-mirsky matrix approximation theorem," *Linear Algebra and its Applications*, vol. 88-89, pp. 317–327, 1987. [Online]. Available: <https://www.sciencedirect.com/science/article/pii/0024379587901145> **IV**
- [37] D. Dowson and B. Landau, "The Frechet distance between multivariate normal distributions," *Journal of Multivariate Analysis*, vol. 12, no. 3, pp. 450–455, 1982. [Online]. Available: <https://www.sciencedirect.com/science/article/pii/0047259X8290077X> **IV**
- [38] S. Boyd, S. P. Boyd, and L. Vandenberghe, *Convex optimization*. Cambridge university press, 2004. **IV**
- [39] W. Ford, *Numerical linear algebra with applications: Using MATLAB*. Academic Press, 2014. **IV**
- [40] A. Papoulis and S. U. Pillai, "Probability, random variables, and stochastic processes," 2002. **VI**
- [41] S. Liu, J. Cheng, and N. C. Beaulieu, "Asymptotic error analysis of diversity schemes on arbitrarily correlated Rayleigh channels," *IEEE Transactions on Communications*, vol. 58, no. 5, pp. 1351–1355, 2010. **VI**
- [42] G. Golub, "Numerical methods for solving linear least squares problems," *Numerische Mathematik*, vol. 7, no. 3, pp. 206–216, 1965. **VI**